A Joint Experimental and Theoretical Study of the Interaction between Aluminum and Electroluminescent Polymers: Cyano Derivatives of Poly(*p*-phenylene vinylene)

M. Fahlman, W. R. Salaneck, S. C. Moratti, A. B. Holmes, and J. L. Brédas*

Abstract: The early stages of metal/polymer interface formation between aluminum and poly(2,5,2′,5′-tetrahexyloxy-8,7′-dicyanodi-*p*-phenylenevinylene) or their ring-substituted derivatives have been studied theoretically by using quantum-chemical calculations as well as experimentally by X-ray photoelectron spectroscopy and ultraviolet photoelectron spectroscopy. This class of conjugated polymer is of interest in the development of organic light-emitting diodes. The theoretical and experimental results indicate that aluminum preferentially reacts with the polymer by forming covalent bonds with the nitrogen and carbon atoms of the cyano groups. When the side chains of the phenylene rings include carbonyl groups, however, the theoretical results indicate that the carbonyl moiety is another preferred site of interaction.

Keywords
light-emitting diodes · polymers · semiempirical calculations · electroluminescence · polymer/metal interface

Introduction

Research activity in the field of conjugated polymers has increased continuously,[1, 2] ever since it was discovered that polyacetylene can be doped to high electrical conductivity.[3] Much effort has been invested into studying the nature of charge storage in both degenerate and nondegenerate ground-state conjugated polymers and model molecular systems.[4–8] In recent years considerable attention has been devoted to the pristine (semiconducting) state of the conjugated polymers, especially because of their potential applications as organic light-emitting diodes (polymer-LEDs),[9–11] field-effect transistors,[12–14] or nonlinear optical materials.[1, 15]

Light-emitting diodes in which thin films of conjugated polymers constitute the active layer were first reported in 1990 by Friend and co-workers, who succeeded in fabricating an LED with poly(*p*-phenylene vinylene) (PPV) as the emission layer, ITO as the hole-injecting electrode, and aluminum as the electron injecting electrode.[9] Interest in this field then grew rapidly, and extensive research was conducted in order to improve both the electroluminescent yield and the variety of colors of these devices. In order to tune the bandgap, and hence color, substituted PPVs, typically poly(dialkoxyphenylene vinylene)s,[10, 16] but also other polymers such as poly(*p*-phenylene)s and poly(alkylthiophene)s,[17] have been used. Methods of improving the electroluminescence efficiency include the use of low work-function electrodes (such as calcium) in order to enhance the electron injection rate,[10] the design of copolymers with conjugated and nonconjugated segments in order to create preferred sites for electron–hole recombination,[9] and the fabrication of multilayered devices.[18] Recently, the derivatization of the polymer backbone by electron-withdrawing substituents such as cyano groups was considered in order to lower the conduction band of the active polymer and, hence, ease the electron injection process with aluminum;[19] in poly(2,5,2′,5′-tetrahexyloxy-8,7′-dicyanodi-*p*-phenylenevinylene), or CN-PPV, a high internal quantum efficiency can indeed be obtained by using aluminum as electron-injecting contact.[20]

The purpose of this work is to describe, by means of a joint experimental and theoretical approach, the early stages of metal/polymer interface formation upon deposition of aluminum on CN-PPV and some derivatives thereof. We also compare our results with those of similar studies carried out on PPV[21, 22] and poly(ethylene terephthalate) (PET).[23] This study has been carried out under the premise that the results should not only be of fundamental chemical and physical interest, but also contribute to an improved design of polymer-based LEDs.

---

[*] M. Fahlman, W. R. Salaneck
Department of Physics, Linköping University
S-581 83 Linköping (Sweden)
J. L. Brédas, M. Fahlman
Service de Chimie des Matériaux Nouveaux
Centre de Recherche en Electronique et Photonique Moléculaires
Université de Mons-Hainaut, B-7000 Mons (Belgium)
Fax: Int. code +(65)37-3366
S. C. Moratti, A. B. Holmes
Melville Laboratory for Polymer Synthesis, Cambridge University
Cambridge CB2 3RA (UK)

0947-6539/97/0302-0286 $ 15.00+.25/0

Experimental and Theoretical Details

Experimental: Both X-ray and ultraviolet photoelectron spectroscopy (XPS and UPS) measurements were carried out in Linköping, on an ultrahigh vacuum (UHV) instrument, of our own design and construction, with a base pressure of better than 10^{-10} Torr. The X-ray source for XPS was unmonochromatized MgK$_{\alpha1\alpha2}$ at $h\nu = 1253.6$ eV. The resolution of the hemispherical electron energy analyzer was set such that the full width at half maximum of the Au(4f$_{7/2}$) line was 0.9 eV. UPS was performed with monochromatized He I ($h\nu = 21.2$ eV) photons from a He-resonance lamp. The energy resolution was set to 0.2 eV for XPS and 0.1 eV for UPS.

Aluminum was deposited on the surfaces of samples held at 20 °C, by using a home-built evaporation source. During deposition, the background pressure rose to only about 10^{-9} Torr. The deposition was carried out in carefully timed steps; the resultant number of Al atoms per phenylene–vinylene unit was estimated from the intensity ratio between the XPS C(1 s) and Al(2 p) core electron intensities (areas under the curves). Two types of samples were used in the experiments: a) the CN-PPV polymer and b) a three-ring oligomer, 3CN-PV (molecular structures shown in Figure 1). The CN-PPV samples were produced by spin-coating from a CHCl$_3$ solution onto SiO$_2$ substrates, and the thin films of 3CN-PV by sublimating the oligomers from a Knudsen cell onto cooled Au substrates.

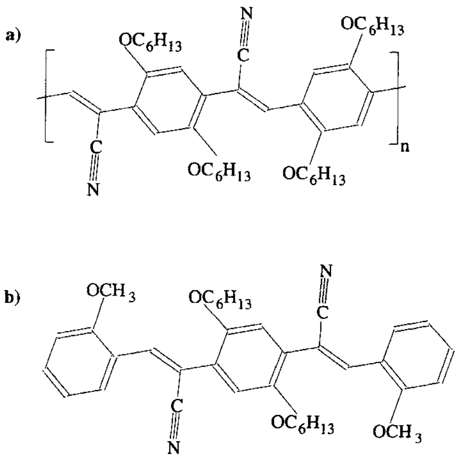

Figure 1. Geometric structures of a) CN-PPV and b) 3CN-PV.

Theoretical: The quantum-chemical calculations were carried out on isolated polymer or oligomer chains. The geometries of the CN-PPV polymer and the 3CN-PV oligomer were optimized using the Austin Model 1 (AM 1) Hamiltonian [24] and used as input into the electronic-structure calculations. It was practical to optimize the geometry of the CN-PPV polymers containing dimethoxy instead of dihexyloxy side chains, since the length of the alkoxy chains does not affect the low binding energy π bands. Interaction with aluminum was modeled with four-ring oligomers of various CN-PPV polymers and two Al atoms. The oligomers used were those corresponding to a) poly(8,7′-dicyanodi-*p*-phenylenevinylene); b) poly(2,5,2′,5′-tetramethyl-8,7′-dicyanodi-*p*-phenylenevinylene); c) poly(2,5,2′,5′-tetramethoxy-8,7′-dicyanodi-*p*-phenylenevinylene); and d) poly(2,5,2′,5′-tetraformyl-8,7′-dicyanodi-*p*-phenylenevinylene). The geometries were fully optimized for all the configurations considered, by means of the AM 1 Hamiltonian. Also, qualitative estimates of the charge distributions in connection with aluminum deposition were obtained by Mulliken population analysis.

Electronic band structure calculations for pristine CN-PPV and 3CN-PV were carried out by the valence effective Hamiltonian method [25,26]; the VEH technique is a nonempirical pseudopotential method based on an effective Fock Hamiltonian. In this case, the polymer chains were taken to be planar (torsion angles set equal to zero), in order to simulate the conformation expected in the solid state. The bare density of valence electronic states (DOVS) curves were computed from the VEH output in the standard way, that is, by taking the inverse of the derivative of the band energies with respect to momentum. In order to make comparison with solid-state UPS data (with the vacuum level taken as reference level), the bare DOVS curves were treated in the usual manner (see, for example, Refs. [26–27]): 1) contraction along the energy scale, 2) a shift to lower binding energies to compensate for solid-state effects, and 3) convolution by a Gaussian to appropriately match the experimental peak broadening in the UPS data. This type of theoretical approach has been used successfully in previous instances, for instance to describe aluminum deposition on poly-*p*-phenylene vinylene [21–22] or polyethyleneterephtalate, polystyrene, and polycaprolactone [23].

Theoretical Results

Poly(8,7′-dicyanodi-*p*-phenylenevinylene): Two Al atoms were allowed to interact near the central unit (Figure 2a) of the four-ring oligomer. Several different configurations were obtained, with the aluminum atoms bonding with the phenylene carbons, vinylene carbons, and/or the carbons and nitrogens of the cyano groups. The three most energetically favored structures are depicted in Figures 2b–d, while the AM 1-optimized bond lengths are displayed in Table 1. The most favored structure is that corresponding to (b), which is 3.8 kcal mol^{-1} lower than (c) and 4.2 kcal mol^{-1} lower than (d). In all cases, the cyano group is the preferred reaction site for aluminum. In a similar study of the interaction of aluminum atoms with PPV,[21] the most favored structure was with two aluminum atoms forming bonds with each of the vinylene carbons within the same vinylene moiety. In the present case, however, this type of structure, with formation of Al–C8 and Al–C9 bonds, was found to be 25.1 kcal mol^{-1} higher in energy than the optimal configuration (b).

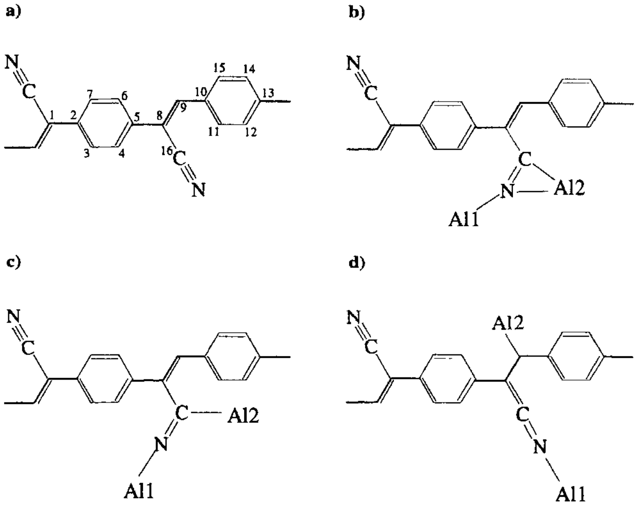

Figure 2. Central section of the four-ring oligomer corresponding to poly(8,7′-dicyanodi-*p*-phenylenevinylene) for: a) the pristine case; and b), c), and d), the three most energetically favored AM 1-optimized structures for the Al$_2$/oligomer complex.

In (b) and (c), both Al atoms bind to the cyano group, and one is attached to the nitrogen; the difference between these two configurations is that there is a C-Al-N bridge in (b), whereas in (c) the second Al atom forms a bond only with the cyano carbon. The C16–N bond (see Table 1) increases in length from 1.164 Å in (a) to 1.319 Å in (b) and to 1.266 Å in (c), with the change from triple-bond to more double-bond character; the C16–N bond in structure (d) is shorter than in (b) and (c) (1.207 Å).

Table 1. AM1-optimized bond lengths (Å) and dihedral angles (°) of the central part of the four-ring oligomer of i) poly(8,7′-dicyanodi-*p*-phenylenevinylene) and ii) poly(2,5,2′,5′-tetramethoxy-8,7′-dicyanodi-*p*-phenylenevinylene) for a) the pristine case and for b), c), and d) the three most energetically favored AM1-optimized structures for the Al_2/oligomer complex as shown in Figures 2 and 4.

	Structure a		Structure b		Structure c		Structure d	
	(i)	(ii)	(i)	(ii)	(i)	(ii)	(i)	(ii)
*r*C1–C2	1.4660	1.4665	1.4662	1.4668	1.4661	1.4662	1.4654	1.4668
*r*C2–C3	1.4022	1.4121	1.4004	1.4124	1.4016	1.4109	1.4035	1.4109
*r*C3–C4	1.3914	1.3987	1.3987	1.4068	1.3920	1.3996	1.3896	1.4056
*r*C4–C5	1.4022	1.3995	1.4076	1.4058	1.4016	1.3989	1.4055	1.4069
*r*C5–C6	1.4019	1.4120	1.4025	1.4129	1.4029	1.4137	1.4115	1.4153
*r*C6–C7	1.3916	1.3989	1.3910	1.3986	1.3912	1.3981	1.3954	1.3962
*r*C5–C8	1.4663	1.4666	1.4734	1.4735	1.4623	1.4621	1.4579	1.4592
*r*C8–C9	1.3507	1.3514	1.3542	1.3578	1.3484	1.3491	1.4910	1.4898
*r*C9–C10	1.4524	1.4514	1.4487	1.4477	1.4620	1.4614	1.4855	1.4861
*r*C10–C11	1.4019	1.3984	1.4019	1.3991	1.4093	1.4070	1.4072	1.4014
*r*C11–C12	1.3911	1.3978	1.3925	1.3983	1.3996	1.4071	1.3906	1.3993
*r*C12–C13	1.4039	1.4160	1.4025	1.4165	1.4000	1.4138	1.4049	1.4153
*r*C13–C14	1.4019	1.3981	1.4029	1.3980	1.4050	1.3998	1.4015	1.3993
*r*C14–C15	1.3910	1.3980	1.3890	1.3976	1.3896	1.3975	1.3921	1.3968
*r*C8–C16	1.4252	1.4259	1.4541	1.4484	1.4978	1.4962	1.3372	1.3375
*r*C3–O1		1.3831		1.3793		1.3840		1.3799
*r*C6–O2		1.3828		1.3824		1.3835		1.3851
*r*C12–O3		1.3821		1.3794		1.3784		1.3822
*r*C15–O4		1.3818		1.3819		1.3812		1.3861
*r*O1–C19		1.4246		1.4269		1.4248		1.4258
*r*O2–C20		1.4247		1.4243		1.4248		1.4236
*r*O3–C21		1.4241		1.4273		1.4274		1.4222
*r*O4–C22		1.4244		1.4246		1.4244		1.4242
*r*C16–N	1.1637	1.1640	1.3189	1.3220	1.2661	1.2670	1.2066	1.2059
*r*Al1–N	–	–	1.7035	1.7009	1.6294	1.6273	1.6565	1.6535
*r*Al2–N	–	–	1.7499	1.7453	2.6635	2.9538	–	–
*r*Al2–C(j)	–	–	1.8077(16)	1.8035(16)	1.8075(16)	1.8031(16)	1.8206(9)	1.8093(9)
∢C9-C8-C5-C4	143	140	123	124	136	137	141	57
∢C11-C10-C9-C8	40	36	20	23	78	75	72	73
∢C10-C9-C8-C7	179	177	179	180	179	176	129	132
∢C12-C11-C10-C9	179	179	180	179	174	174	177	177

The variation in the C16–N bond length can be explained by looking at the bonding in the different structures. In structure (b), the Al1–N bond is mostly formed through the overlap of the s and p_x orbitals of Al1 with the p_x orbitals of the nitrogen atom. The C16–Al2 bond is formed through the overlap of the p_y orbitals of C16 and the s and p_y orbitals of Al2. The N–C16 bond is mostly of σ-bonding nature, though there exists p_z overlap between N and C16; this overlap, however, is much weaker than in structures (c) and (d). There is also some p_z overlap along Al1-N-Al2 and Al1-N-C16-Al2 as well. In structure (c), the N–Al1 bond is formed through overlap of the respective atoms p_y orbitals (σ-bonding). The C16–Al2 bond is obtained through overlap of the p_x orbitals. As in (b), there is some p_z overlap along Al1-N-C16-Al2. The p_z overlap between C16–N, though stronger than in (b), is still not of the same order as that of a pure C=N bond as calculated by means of the AM1 Hamiltonian, hence the longer bond length (1.266 Å) compared to formimide (1.228 Å). The p_z overlap between Al1 and N is stronger for (c) than (b), hence the shorter N–Al1 bond length. In structure (d), the C9–Al2 bond is formed by overlap between the p_y orbitals of C9 and the s and p_y orbitals of Al2. The N–Al1 bond is mostly formed by p_z–p_z overlap. Note that in structure (d) there is no significant p_z overlap along Al1-N-C16-C8, owing to the nodes between either N and C16 or C16 and C8. The p_z–p_z overlap in the C16–C8 and N–C16 bonds are much stronger in structure (d) than in (b) and (c), which is consistent with the comparatively shorter bond lengths.

It is worth pointing out that the conjugation along the polymer backbone in cases (b) and (c) is not broken *directly* by the interactions with the Al atoms. However, the Al–cyano complexes that are formed induce large ring torsion angles (see Table 1), which cause the overlap of the π-electron wavefunctions along the backbone to be decreased significantly (at least along isolated chains; in the solid state, packing effects are expected to reduce the torsions). In case (c), the cyano–aluminum complex is rotated by nearly 30° out of the C16-C8-C9 plane; this minimizes the steric interaction between the Al2 atom and the hydrogen atoms of the adjacent phenylene ring. In case (d), the conjugation is broken directly, since one of the Al atoms binds to the carbon atom of a vinylene group, and the other Al atom forms a bond with the nitrogen of the cyano group; the direct break of π conjugation is evident from the bond length values: the C8–C9 bond increases from 1.351 to 1.491 Å, and the C9 carbon assumes an sp^3 bonding configuration.

The decrease in overlap of the π-electron wavefunctions along the backbone for structures (b) and (c), combined with the break of π conjugation for structure (d), prevent the choice of optimal configuration for comparison with experimental (UPS) data. Indeed, in all cases the highest valence (and lowest conduction) bands, which are dispersed in the pristine case, become flatter upon metalization.

Instead, the charge transfer induced by the aluminum deposition was studied using Mulliken population analysis in order to make a qualitative comparison with the chemical shifts obtained in XPS core level spectra. In all the configurations, the nitrogen atom receives about $0.5|e|$ added charge. For configuration (b), carbon atoms 8 and 16 gain about 0.17 and $0.11|e|$, respectively, with the charge on carbon atom 9 basically unaffected. For case (c), carbons 8 and 16 gain 0.11|*e*| and carbon 9 gains 0.08|*e*|. In case (d), carbon atom 8 gains 0.25|*e*| but atom 16 loses 0.30|*e*|, in contrast to the situation in the (b) and (c) structures where the $p_z - p_z$ overlap of N–C16 and C16–C8 is substantially smaller; carbon atom 9 gains 0.34|*e*|, since one of the Al atoms binds to it. Each Al atom transfers about 0.35–0.50 to the molecule, with the largest charge transfer taking place for configuration (d), and the smallest for (b).

Poly(2,5,2′,5′-tetramethyl-8,7′-dicyanodi-*p*-phenylenevinylene): The central unit of the four-ring oligomer of poly(2,5,2′,5′-tetramethyl-8,7′-dicyanodi-*p*-phenylenevinylene) is depicted in Figure 3a; the three most energetically favored structures for two aluminum atoms interacting with this central unit are shown in Figures 3b–d. Structure (b) is the lowest in energy, 3.7 kcal mol^{-1} lower than (c) and 4.7 kcal mol^{-1} lower than (d). As can be seen from the figures, it is evident that the addition of the methyl groups does not affect the aluminum interaction with these polymers. In fact, the same type of bonds are formed with nearly identical bond lengths, and these are therefore not given in Table 1. In structure (c), the cyano–aluminum complex is rotated by about 25° out of the C16-C8-C9 plane, similar to the case for poly(8,7′-dicyanodi-*p*-phenylenevinylene). The structure with the fourth lowest energy was that in which the aluminum atoms form bonds with the vinylene carbons, Al–C8 and Al–C9. This structure was 22.7 kcal mol^{-1} higher in energy than (b).

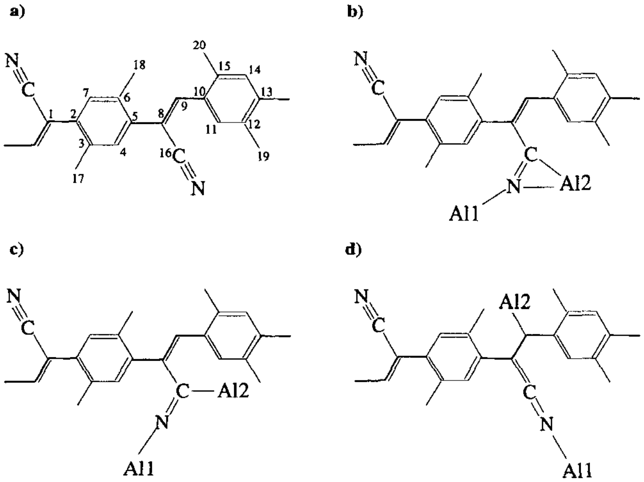

Figure 3. Illustration of the central part of the four-ring oligomer of poly(2,5,2′,5′-tetramethyl-8,7′-dicyanodi-*p*-phenylenevinylene) for: a) the pristine case; and b), c), and d), the three most energetically favored AM1-optimized structures for the Al_2/oligomer complex.

The Mulliken population analysis shows charge transfers nearly identical to those in the corresponding structures of poly(8,7′-dicyanodi-*p*-phenylenevinylene), reinforcing the point that the methyl groups do not affect the nature of the interaction of aluminum atoms with the polymer. These results are consistent with the absence of significant interactions upon deposition of aluminum on polyethylene.[28]

Poly(2,5,2′,5′-tetramethoxy-8,7′-dicyanodi-*p*-phenylenevinylene): In Figure 4, the central unit of poly(2,5,2′,5′-tetramethoxy-8,7′-dicyanodi-*p*-phenylenevinylene) is illustrated (Figure 4a) together with the three most energetically favored structures for interaction with two aluminum atoms (Figures 4b–d). Again, the formation of the C-Al-N complex of (b) is the lowest in energy, (c) being 6.3 and (d) 6.7 kcal mol^{-1} higher. Here also, the bond lengths (given in Table 1) of the different structures are very close to those of aluminum interacting with poly(8,7′-dicyanodi-*p*-phenylenevinylene).

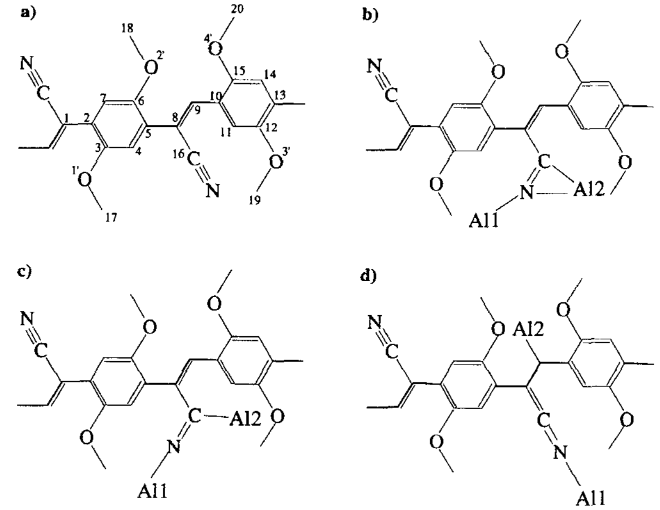

Figure 4. Illustration of the central part of the four-ring oligomer of poly(2,5,2′,5′-tetramethoxy-8,7′-dicyanodi-*p*-phenylenevinylene) for: a) the pristine case; and b), c), and d), the three most energetically favored AM1-optimized structures for the Al_2/oligomer complex.

The cyano–aluminum complex in structure (c) is rotated by about 35° out of the C16-C8-C9 plane, and the C9 carbon of structure (d) becomes sp^3 hybridized. Note that, owing to inter-ring torsion and rotation of the cyano–aluminum complex in (c), the Al atoms are not situated as close to the methoxy groups as the (two-dimensional) figures might suggest. Like the methyl groups, the methoxy substituents do not significantly affect the aluminum interaction with the polymer, nor is the aluminum/oxygen interaction likely. In fact, the aluminum atoms did not form bonds with the methoxy oxygens in any of the minimum energy structures obtained from the present calculations. For the case of dimethoxy-substituted PPV,[21] it also was found that aluminum/ether oxygen interactions are not favorable.

The Mulliken population analysis is qualitatively the same as in the previous polymers. Hence, neither alkyl nor alkoxy substituents on the phenylene rings appear to affect the interaction of aluminum atoms with the polymer.

Poly(2,5,2′,5′-tetraformyl-8,7′-dicyanodi-*p*-phenylenevinylene): The middle two rings of the four-ring oligomer of poly(2,5,2′,5′-tetraformyl-8,7′-dicyanodi-*p*-phenylenevinylene) is depicted in Figure 5a. The main reason for studying this polymer, which has not been synthesized, is that carbonyl moieties are expected to be formed upon oxidation of the pristine polymer.[11] Upon metalization, we note striking dissimilarities compared to the previous three polymers. The most favored structure for the interaction with two aluminum atoms is that shown in Figure 5b, where one aluminum atom reacts with a formyl oxygen,

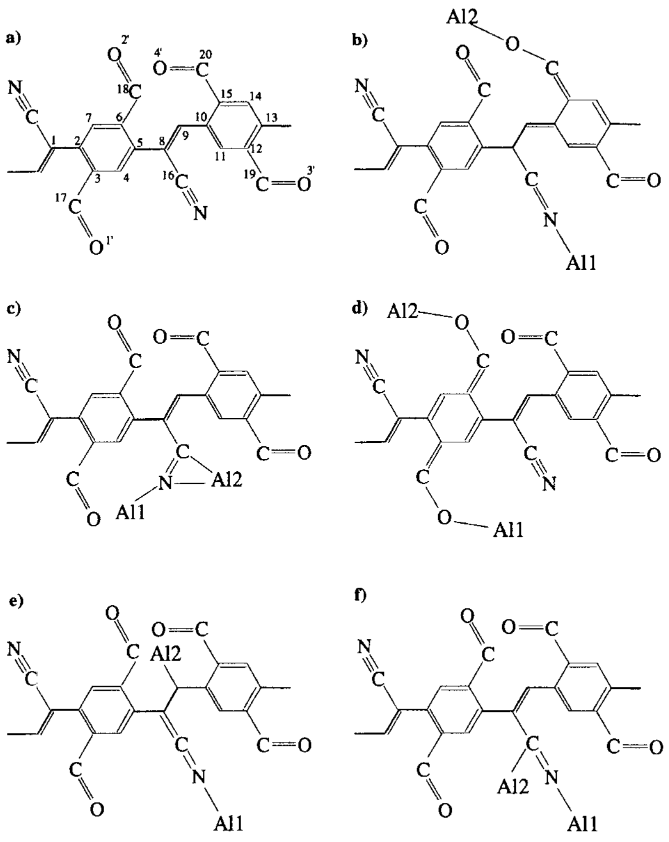

Figure 5. Illustration of the central part of the four-ring oligomer of poly(2,5,2',5'-tetraformyl-8,7'-dicyanodi-*p*-phenylenevinylene) for : a) the pristine case; and b), c), d), e), and f), the five most energetically favored AM1-optimized structures for the Al_2/oligomer complex.

Table 2. AM1-optimized bond lengths (Å) and dihedral angles (°) of the central part of the pristine four-ring oligomer of poly(2,5,2',5'-tetraformyl-8,7'-dicyanodi-*p*-phenylenevinylene) (a) and of the Al_2/oligomer complexes b), c), d), e), and f) illustrated in Figure 5.

	a	b	c	d	e	f
*r*C1–C2	1.4725	1.4727	1.4721	1.4740	1.4706	1.4723
*r*C2–C3	1.4039	1.4045	1.4007	1.4571	1.4021	1.4016
*r*C3–C4	1.3993	1.3984	1.4058	1.4466	1.4037	1.4037
*r*C4–C5	1.3992	1.4010	1.4062	1.3560	1.4079	1.4076
*r*C5–C6	1.4041	1.4051	1.4073	1.4571	1.4095	1.4057
*r*C6–C7	1.3989	1.4000	1.3976	1.4470	1.3966	1.3978
*r*C5–C8	1.4724	1.4668	1.4752	1.4738	1.4634	1.4793
*r*C8–C9	1.3482	1.4487	1.3523	1.3484	1.4890	1.3432
*r*C9–C10	1.4563	1.3722	1.4555	1.4561	1.4851	1.4579
*r*C10–C11	1.4009	1.4492	1.4012	1.4020	1.4064	1.4015
*r*C11–C12	1.3984	1.3623	1.3990	1.3977	1.3979	1.3978
*r*C12–C13	1.4083	1.4516	1.4070	1.4087	1.4088	1.4090
*r*C13–C14	1.4010	1.3646	1.4012	1.4002	1.3999	1.4001
*r*C14–C15	1.3981	1.4426	1.3976	1.3988	1.3980	1.3993
*r*C8–C16	1.4249	1.3421	1.4578	1.4265	1.3386	1.4985
*r*C3–C19	1.4815	1.4813	1.4853	1.3672	1.4836	1.4843
*r*C6–C20	1.4813	1.4779	1.4828	1.3670	1.4776	1.4825
*r*C12–C21	1.4789	1.4774	1.4811	1.4785	1.4782	1.4781
*r*C15–C22	1.4785	1.3787	1.4785	1.4779	1.4804	1.4774
*r*C19–O1'	1.2319	1.2321	1.2314	1.3322	1.2321	1.2313
*r*C20–O2'	1.2318	1.2330	1.2316	1.3321	1.2324	1.2318
*r*C21–O3'	1.2321	1.2320	1.2323	1.2323	1.2326	1.2320
*r*C22–O4'	1.2322	1.3211	1.2326	1.2319	1.2309	1.2324
*r*C16–N	1.1639	1.2033	1.3167	1.1640	1.2031	1.2620
*r*Al1–N	–	1.6669	1.7086	–	1.6648	1.6301
*r*Al2–N	–	–	1.7520	–		2.7520
*r*Al2–C(i)	–	–	1.8045(9)	–	1.8216(9)	1.8285(9)
*r*Al1–O(j)	–	–	–	1.7048(1')	–	–
*r*Al2–O(k)	–	1.7382(4')	–	1.7044(2')	–	–
∢C9-C8-C5-C4	108	104	114	112	65	107
∢C11-C10-C9-C8	46	9	36	45	73	57
∢C10-C9-C8-C7	178	129	179	177	130	174
∢C12-C11-C10-C9	178	155	180	178	177	177

and the other Al atom forms a bond with the nitrogen atom. In this case, the π conjugation is broken directly, since the bonds in both the vinylene group and the phenylene ring become severely distorted, as can be seen from Table 2 and Figure 5b. For structure (c), which is only 1.8 kcal mol^{-1} higher in energy, we have the familiar C-Al-N complex, which induces large inter-ring torsion angles, again severely decreasing the conjugation along the backbone. The bond lengths are approximately the same as for the corresponding structures of the previous polymers. Structure (d) is 3.9 kcal mol^{-1} higher in energy than (b). Here, both aluminum atoms form bonds with the oxygens of the formyl groups on the same phenylene ring. This disrupts the π conjugation of that particular ring, but the vinylene groups and the other rings remain unaffected. Structures (e) and (f) are similar to the corresponding configurations obtained for the previous three polymers, but here the stability order is reversed; structure (e) is lower in energy than (f); (e) and (f) are 5.8 and 7.9 kcal mol^{-1} higher than (b), respectively. In contrast to alkyl or alkoxy substitutions, the formyl groups are thus found to strongly affect the nature of the interaction with two aluminum atoms. For diformyl-substituted PPV,[21] the most favored structure also involved an Al-O-C complex. These results are consistent with the well-established reactivity of aluminum towards carbonyl groups, for instance in polyimide[29] or PET.[23]

Upon interaction with two aluminum atoms, C8 and C9 in structure (b) gain 0.24|e| and 0.10|e|, respectively; carbon atom 16 loses 0.31|e|, the nitrogen atom gains 0.51|e|, the formyl carbon gains 0.08|e|, and the oxygen atom gains 0.17|e|; the aluminum atom forming a bond to the nitrogen donates 0.55|e|, whereas the other Al atom donates 0.44|e|. In structure (d), the two oxygen atoms forming bonds with the aluminum each gain 0.23|e|, the formyl carbon atoms each gain 0.10|e|, and the Al atoms lose 0.47|e| each. The charge transfers in structures (c), (e), and (f) are qualitatively the same as in the equivalent structures for the previous three oligomers.

Experimental Results

In order to make a comparison with experiment, the early stages of formation of the interface between aluminum and poly-(2,5,2',5'-tetrahexyloxy-8,7'-dicyanodi-*p*-phenylenevinylene) (CN-PPV) and a three-ring oligomer thereof (3CN-PV) were studied. For these compounds, the theoretical results indicate three likely structures. With their energy difference of less than 7 kcal mol^{-1}, it is difficult to discriminate between them on the basis of theory alone, hence the importance of gathering experimental results that are as accurate as possible. We first look at the interface formation between aluminum and 3CN-PV in detail, and then use these results when discussing the aluminum/CN-PPV interaction.

The UPS HeI and HeII spectra for 3CN-PV are compared with the VEH-derived DOVS in Figure 6. The experimental spectra are well resolved and in good agreement with theory,

0947-6539/97/0302-0290 $ 15.00+.25/0

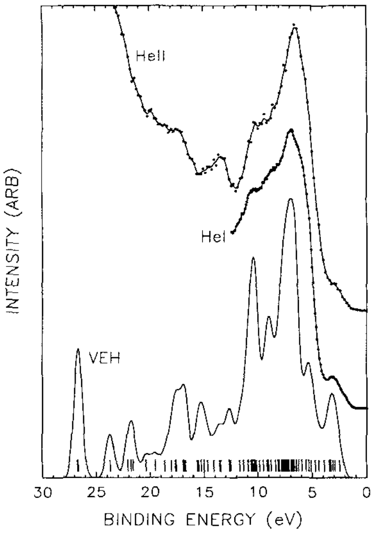

Figure 6. HeI and HeII UPS spectra, as well as the corresponding occupied energy bands and the DOVS calculated by the VEH method, for 3CN-PV, with the Fermi level as reference.

evidence that the material is of good quality (minimum of chemical and spatial inhomogeneity). The spectral features between 1 and 4 eV are derived from π bands; the highest-lying state (closest to the Fermi level) derives from wavefunctions delocalized along the oligomer backbone and those around 3 eV, from wavefunctions localized on the phenylene rings. The structure between 5–10 eV in the UPS spectrum is derived mostly from σ states, mainly from the C–H bonds of the hexyloxy chains. The peak at 10.5 eV is derived from oxygen lone pair states. The peaks between 12 and 25 eV are derived from σ states, with the peak at 26.5 eV arising from O(2s) states.

In the XPS core level spectra, no excess amount of oxygen nor any indication of foreign substances were observed. As mentioned above, large charge transfer between aluminum atoms and the oligomers/polymers show up in the XPS core level spectra as chemical shifts. If the atoms gain electronic (negative) charge, the corresponding XPS spectral line (peak) moves toward lower binding energies (closer to the Fermi level); for a loss of electronic charge, the opposite is true. According to the results presented for poly(2,5,2′,5′-tetramethoxy-8,7′-dicyanodi-p-phenylenevinylene), structures (b) and (c) experience approximately the same overall charge transfer, whereas structure (d) shows strong dissimilarities. Hence, it is possible to differentiate between structures (b) and (c) on the one hand, and (d) on the other, by studying the XPS core level spectra.

The calculations show that the nitrogen atoms gain approximately $0.5|e|$ from the aluminum atoms, and this should be related to a large shift of the N(1s) peak towards lower binding energies. In Figure 7 (left), we show the N(1s) spectrum of pristine 3CN-PV; the binding energy of the peak is 400.0 eV.

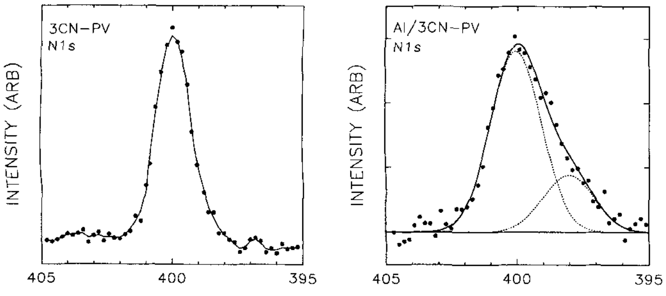

Figure 7. XPS N(1s) spectra, with the Fermi level taken as reference. Left: pristine 3CN-PV; right: Al/3CN-PV at a metalization level of approximately two Al atoms per oligomer.

When aluminum is deposited on the sample, a shoulder immediately appears on the low binding energy side of the main peak and grows in intensity with increasing deposition of aluminum. At an aluminum deposition in excess of about two Al atoms per phenylene–vinylene unit, a low binding energy shoulder, centered near 398.0 eV, is clearly visible in the N(1s) spectrum shown in Figure 7 (right). This is a clear indication that (some of) the nitrogen atoms of the cyano groups do indeed react with the Al atoms. Note that the main peak at 400.0 eV still remains, since XPS probes depths of up to 100 Å, and the Al atoms remain in the near-surface region according to studies using angle-dependent XPS.

Figure 8 (left) shows the C(1s) spectrum of pristine 3CN-PV. The main peak at 285.2 eV consists of contributions from the alkyl carbons of the hexyloxy chains and the unsaturated carbons of the phenylene and vinylene groups. The shoulder at 286.8 eV consists of contributions from the C–O carbons of the hexyloxy side chains and phenylene groups as well as from the C≡N carbons, in agreement with published results which indicate that the binding energy difference between C–C,H carbons and C–O carbons is about 1.5–1.6 eV.[23] The results of a study on polyacrylonitrile[30] indicate that the chemical shift of C≡N carbons is ca. 1.7 eV relative to C–C,H. Therefore, in cases (b) and (c), a shoulder on the low binding energy side of the C(1s) peak is expected in connection with the deposition of aluminum, because of the charge added on the C8 and C16 carbon atoms and a decrease in relative intensity of the high binding energy shoulder, since the C16 carbon atoms then no longer contribute to the intensity. For case (d), a larger shift, and hence a more pronounced shoulder at low binding energies, associated with the addition of charge to the C8 and C9 carbon atoms, is expected. In addition, a slight increase in the relative intensity of the high binding energy shoulder, as well as a significant broadening, should occur because of the decreased electronic charge density on carbon atom C16.

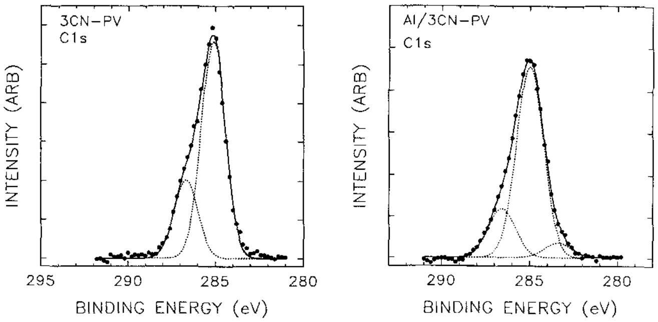

Figure 8. XPS C(1s) spectra, with the Fermi level taken as reference. Left: pristine 3CN-PV; right: Al/3CN-PV at a metalization level of approximately two Al atoms per oligomer.

In Figure 8 (right), we display the C(1s) spectrum taken at the same aluminum coverage as for Figure 7 (right). As can be observed, a new feature has appeared as a shoulder at 283.6 eV. Also, the relative intensity of the shoulder on the high binding energy side of the main peak has decreased (compared to the pristine case). No broadening is seen; on the contrary, the shoulder has moved in somewhat towards the main peak. This suggests that configuration (d) is not likely, while the evolution is consistent with configurations (b) and (c). The shoulder at 283.6 eV represents a chemical shift of 1.6 eV relative to the main peak. This value is smaller than those reported for aluminum atoms covalently bonded to α-sexithiophene molecules (2.5 eV[31]) and PET ($\approx$2.4–2.6 eV[23]). In the latter case, the charge transfer was also calculated by means of a Mulliken population analysis, with the C–Al carbons accepting roughly $0.45|e|$. This also suggests that configurations (b) and (c) are more likely, since the calculated charge transfer in these cases is smaller than that of case (d); hence, smaller chemical shifts are expected.

The valence band electronic structure of CN-PPV has been discussed elsewhere.[32] Results similar to the 3CN-PV case were obtained when the aluminum interface formation with CN-PPV was studied. This is expected since the interaction between the Al atoms and the oligomer/polymer chains are of local character. In Figure 9 (left), the N(1 s) spectrum of pristine CN-PPV is depicted, and Figure 9 (right) shows the N(1 s) spectrum taken at an aluminum concentration of approximately two Al atoms per phenylene–vinylene unit. The binding energy of the main peak as well as that of the low binding energy shoulder are identical with the case of 3CN-PV. Hence, it is again concluded that the Al atoms interact strongly with the cyano nitrogen atoms of the polymer.

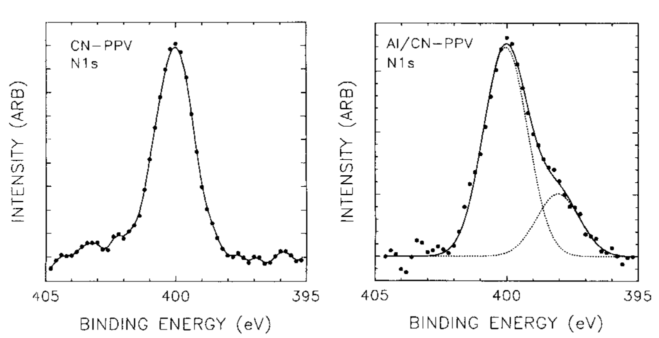

Figure 9. XPS N(1 s) spectra, with the Fermi level taken as reference. Left: pristine CN-PPV; right: Al/CN-PPV at a metalization level of approximately two Al atoms per oligomer.

Figure 10 (left) provides the C(1 s) spectrum of pristine CN-PPV, and Figure 10 (right) shows the C(1 s) spectrum taken at the same aluminum coverage as for Figure 9 (right). Here too, the binding energies as well as the evolution of the new features upon aluminum deposition are nearly identical to those of the 3CN-PV case. As a result, structures (b) and (c), where the aluminum atoms react with the cyano groups, are those most likely to occur at the early stages of interface formation on CN-PPV.

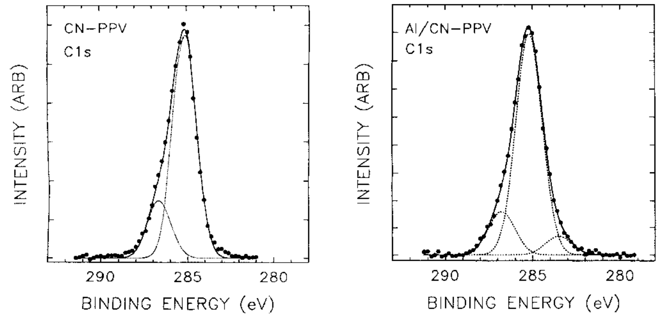

Figure 10. XPS C(1 s) spectra, with the Fermi level taken as reference. Left: pristine CN-PPV; right: Al/CN-PPV at a metalization level of approximately two Al atoms per oligomer.

Summary and Conclusions

The early stages of aluminum interface formation on a cyano-substituted poly(*p*-phenylene vinylene), of current interest for applications in polymer light-emitting devices, have been studied by using a combined theoretical and experimental approach. Both a model oligomer as well as the actual polymer have been studied experimentally, and a variety of possible structures has been considered theoretically.

The model calculations indicate that, for poly(8,7′-dicyanodi-*p*-phenylenevinylene), poly(2,5,2′,5′-tetraalkyl-8,7′-dicyanodi-*p*-phenylenevinylene)s, and poly(2,5,2′,5′-tetraalkoxy-8,7′-dicyanodi-*p*-phenylenevinylene)s, aluminum atoms preferentially react with the cyano groups in pairs, one forming a covalent bond with the nitrogen atom, the other forming either a N-Al-C complex with the same cyano group, or forming a covalent bond with the cyano carbon. The dialkyl and dialkoxy ring substitutions do not appear to affect the nature of the interaction of aluminum atoms with the molecules considered. When carbonyl groups are present as ring substituents, however, other structures, involving mainly covalent bonds between the aluminum atoms and the carbonyl oxygens, become possible as well.

Acknowledgements: The authors are grateful to Prof. R. H. Friend, Dr. R. Lazzaroni, and Dr. M. Lögdlund for fruitful collaboration. The Linköping-Mons collaboration is supported by the European Commission (within the ESPRIT program – project 8013 LEDFOS and Human Capital and Mobility program). In addition, research on conjugated polymers in Linköping is supported in general by grants from the Swedish Natural Sciences Research Council (NFR), the Swedish National Technical Research Board (TFR), Philips, and Hoechst. Work on conjugated polymers in Mons is supported by the Belgian Federal Government (SSTC) "Pôle d'Attraction Interuniversitaire en Chimie Supramoléculaire et Catalyse", the Belgian National Fund for Scientific Research FNRS/FRFC, and an IBM Academic Joint Study.

Received: July 3, 1996 [F408]

---

[1] a) *Handbook of Conducting Polymers* (Ed.: T. A. Skotheim), Marcel Dekker, New York, **1986**; b) *Conjugated Polymers: The Novel Science and Technology of Highly Conducting and Nonlinear Optically Active Materials* (Eds.: J. L. Brédas, R. Silbey), Kluwer, Dordrecht, **1991**.

[2] *Conjugated Polymers and Related Materials* (Eds.: W. R. Salaneck, I. Lundström, B. Rånby), Proceedings of the Eighty-First Nobel Symposium, Oxford University Press, New York, **1993**; *Handbook of Conducting Polymers* (Eds.: T. A. Skotheim, J. R. Reynolds, R. L. Elsenbaumer), Marcel Dekker, New York, **1996**.

[3] C. K. Chiang, C. R. Fincher, Y. W. Park, A. J. Heeger, H. Shirakawa, E. J. Louis, S. C. Gau, A. G. MacDiarmid, *Phys. Rev. Lett.* **1977**, *39*, 1098.

[4] A. J. Heeger, S. Kivelson, J. R. Schrieffer, W. P. Su, *Rev. Mod. Phys.* **1988**, *60*, 781.

[5] M. Lögdlund, R. Lazzaroni, S. Stafström, W. R. Salaneck, J. L. Brédas, *Phys. Rev. Lett.* **1989**, *63*, 1841; M. Lögdlund, P. Dannetun, S. Stafström, W. R. Salaneck, M. G. Ramsey, C. W. Spangler, C. Fredriksson, J. L. Brédas, *Phys. Rev. Lett.* **1993**, *70*, 970.

[6] M. Fahlman, D. Beljonne, M. Lögdlund, R. H. Friend, A. B. Holmes, J. L. Brédas, W. R. Salaneck, *Chem. Phys. Lett.* **1993**, *214*, 327.

[7] E. Ehrenfreund, D. Moses, K. Lee, A. J. Heeger, J. Cornil, J. L. Brédas, *Chem. Phys. Lett.* **1992**, *196*, 84.

[8] M. G. Ramsey, D. Steinmüller, F. P. Netzer, *Phys. Rev. B* **1990**, *42*, 5902.

[9] J. H. Burroughes, D. D. C. Bradley, A. R. Brown, R. N. Marks, K. Mackay, R. H. Friend, P. L. Burns, A. B. Holmes, *Nature* **1990**, *347*, 539; P. L. Burn, A. B. Holmes, A. Kraft, D. D. C. Bradley, A. R. Brown, R. H. Friend, R. W. Gymer, *Nature* **1992**, *356*, 47.

[10] D. Braun, A. J. Heeger, *Appl. Phys. Lett.* **1991**, *58*, 1982.

[11] N. C. Greenham, R. H. Friend, *Solid State Phys.* **1996**, *49*, 1; W. R. Salaneck, S. Stafström, J. L. Brédas, *Conjugated Polymer Surfaces and Interfaces*, Cambridge University Press, Cambridge, **1996**.

[12] J. H. Burroughes, R. H. Friend, in Ref. [1 b], p. 555; J. H. Burroughes, C. A. Jones, R. H. Friend, *Nature* **1988**, *335*, 137.

[13] A. Assadi, C. Svensson, M. Willander, O. Inganäs, *Appl. Phys. Lett.* **1988**, *53*, 195.

[14] F. Garnier, G. Horowitz, X. Peng, D. Fichou, *Adv. Mater.* **1990**, *2*, 592.

[15] *Nonlinear Optical Properties of Polymers* (Eds.: A. J. Heeger, J. Orenstein, D. R. Ulrich), Materials Research Society, Pittsburgh, **1988**.

[16] D. Braun, A. J. Heeger, H. Kroemer, *J. Electron. Mater.* **1991**, *20*, 945.

[17] G. Grem, G. Leditzky, B. Ullrich, G. Leising, *Synth. Met.* **1992**, *51*, 383; Y. Ohmori, M. Uchida, K. Muro, K. Yoshino, *Jpn. J. Appl. Phys.* **1991**, *30*, 1938; F. Garten, A. R. Schlatmann, R. E. Gill, J. Vrijmoeth, T. M. Klapwijk, G. Hadziioannou, *Appl. Phys. Lett.* **1995**, *66*, 2540.

[18] A. R. Brown, N. C. Greenham, J. H. Burroughes, D. D. C. Bradley, R. H. Friend, P. L. Burn, A. Kraft, A. B. Holmes, *Chem. Phys. Lett.* **1992**, *200*, 46.

[19] S. C. Moratti, D. D. C. Bradley, R. Cervini, R. H. Friend, N. C. Greenham, A. B. Holmes, *SPIE Proceedings Series* **1994**, *2144*, 108; J. L. Brédas, A. J. Heeger, *Chem. Phys. Lett.* **1994**, *217*, 507.

[20] N. C. Greenham, S. C. Moratti, D. D. C. Bradley, R. H. Friend, A. B. Holmes, *Nature* **1993**, *365*, 628.

[21] M. Lögdlund, J. L. Brédas, *J. Chem. Phys.* **1994**, *101*, 4357.

[22] P. Dannetun, M. Lögdlund, M. Fahlman, M. Bohman, S. Stafström, R. Lazzaroni, C. Fredriksson, J. L. Brédas, S. Graham, R. H. Friend, A. B. Holmes, R. Zamboni, C. Taliani, W. R. Salaneck, *Synth. Met.* **1993**, *55–57*, 212.

[23] A. Calderone, R. Lazzaroni, J. L. Brédas, Q. T. Lee, J. J. Pireaux, *J. Chem. Phys.* **1995**, *102*, 4299; A. Calderone, R. Lazzaroni, J. L. Brédas, unpublished results.

[24] M. J. S. Dewar, E. G. Zoebish, R. F. Healy, J. J. P. Stewart, *J. Am. Chem. Soc.* **1985**, *107*, 3902.

[25] J. L. Brédas, R. R. Chance, R. Silbey, G. Nicolas, P. Durand, *J. Chem. Phys.* **1981**, *75*, 255.

[26] J. M. André, J. Delhalle, J. L. Brédas, *Quantum Chemistry Aided Design of Organic Polymers*, World Scientific, Singapore, **1991**.

[27] M. Fahlman, M. Lögdlund, S. Stafström, W. R. Salaneck, R. H. Friend, P. L. Burn, A. B. Holmes, K. Kaeriyama, Y. Sonoda, O. Lhost, F. Meyers, J. L. Brédas, *Macromolecules* **1995**, *28*, 1959.

[28] J. J. Pireaux, unpublished data.

[29] P. S. Ho, P. O. Hahn, J. W. Bartha, G. W. Rubloff, F. K. LeGoues, B. D. Silverman, *J. Vac. Sci. Tech.* **1985**, *A3*, 739; J. J. Pireaux, M. Vermeersch, C. Gregoire, P. A. Thiry, R. Caudano, T. C. Clarke, *J. Chem. Phys.* **1988**, *88*, 3353.

[30] C. R. Wu, W. R. Salaneck, J. J. Ritsko, J. L. Brédas, *Synth. Met.* **1986**, *16*, 147.

[31] P. Dannetun, M. Boman, S. Stafström, W. R. Salaneck, R. Lazzaroni, C. Fredriksson, J. L. Brédas, R. Zamboni, C. Taliani, *J. Chem. Phys.* **1993**, *99*, 664.

[32] M. Fahlman, P. Bröms, D. A. dos Santos, S. C. Moratti, N. Johansson, K. Xing, R. H. Friend, A. B. Holmes, J. L. Brédas, W. R. Salaneck, *J. Chem. Phys* **1995**, *102*, 8167.